Highly Efficient Phosphodiester Hydrolysis Promoted by a Dinuclear Copper(II) Complex

Tamás Gajda,*,†,‡,§ Yvonne Düpre,|| Ibolya Török,⊥ Jeffrey Harmer,# Arthur Schweiger,# Jürgen Sander,|| Dirk Kuppert,|| and Kaspar Hegetschweiler*,||,▽

Department of Inorganic and Analytical Chemistry, University of Szeged, P.O. Box 440, H-6701 Szeged, Hungary, Anorganisch-Chemisches Institut der Universität Münster, Wilhelm-Klemm Strasse 8, D-48149 Münster, Germany, Anorganische Chemie, Universität des Saarlandes, Postfach 15 11 50, D-66041 Saarbrücken, Germany, Biocoordination Chemistry Research Group of the Hungarian Academy of Sciences, University of Szeged, P.O. Box 440, H-6701 Szeged, Hungary, and Laboratory of Physical Chemistry, ETH Hoenggerberg, CH-8093 Zuerich, Switzerland

Received June 1, 2000

The interaction of Cu^{II} with the ligand tdci (1,3,5-trideoxy-1,3,5-tris(dimethylamino)-*cis*-inositol) was studied both in the solid state and in solution. The complexes that were formed were also tested for phosphoesterase activity. The pentanuclear complex $[Cu_5(tdciH_{-2})(tdci)_2(OH)_2(NO_3)_2](NO_3)_4 \cdot 6H_2O$ consists of two dinuclear units and one trinuclear unit, having two shared copper(II) ions. The metal centers within the pentanuclear structure have three distinct coordination environments. All five copper(II) ions are linked by hydroxo/alkoxo bridges forming a Cu_5O_6 cage. The Cu−Cu separations of the bridged centers are between 2.916 and 3.782 Å, while those of the nonbridged metal ions are 5.455−5.712 Å. The solution equilibria in the Cu^{II}−tdci system proved to be extremely complicated. Depending on the pH and metal-to-ligand ratio, several differently deprotonated mono-, di-, and trinuclear complexes are formed. Their presence in solution was supported by mass, CW, and pulse EPR spectroscopic study, too. In these complexes, the metal ions are presumed to occupy tridentate $\{O_{ax},N_{eq},O_{ax}\}$ coordination sites and the O-donors of tdci may serve as bridging units between two metal ions. Additionally, deprotonation of the metal-bound water molecules may occur. The dinuclear Cu_2LH_{-3} species, formed around pH 8.5, provides outstanding rate acceleration for the hydrolysis of the activated phosphodiester bis(4-nitrophenyl)-phosphate (BNPP). The second-order rate constant of BNPP hydrolysis promoted by the dinuclear complex (T = 298 K) is 0.95 M^{-1} s^{-1}, which is ca. 47600-fold higher than that of the hydroxide ion catalyzed hydrolysis (k_{OH}). Its activity is selective for the phosphodiester, and the hydrolysis was proved to be catalytic. The proposed bifunctional mechanism of the hydrolysis includes double Lewis acid activation and intramolecular nucleophilic catalysis.

Introduction

A large number of phosphoesterases are activated by two or three metal ions.[1] During the last 10 years, extensive studies have been carried out to elucidate the role of metal ions in the hydrolytic mechanisms. Besides the crystallographic and kinetic studies of native enzymes,[1] low molecular weight functional model systems, mainly metal complexes, have also attracted great interest from a mechanistic point of view.[2−6] The detailed investigation of such complexes was later elaborated to develop artificial nucleases. Oligonucleotide conjugates of highly active metal complexes would potentially be capable of hydrolyzing RNA or DNA in a sequence specific manner and could thus have important applications in biotechnology and chemotherapy.[5]

In order to develop functional phosphodiesterase models based on transition metal complexes we have investigated the hydrolysis of bis(4-nitrophenyl)phosphate (BNPP) and 2,4-dinitrophenyl ethyl phosphate (DNPEP) promoted by the Cu^{II} complexes of 1,3,5-trideoxy-1,3,5-tris(dimethylamino)-*cis*-inositol (tdci). Cyclohexane-based polyamino polyalcohols have been shown to possess several unique coordination properties,[7] at least

* Authors to whom correspondence should be addressed.
† University of Szeged.
‡ Anorganisch-Chemisches Institut der Universität Münster.
§ E-mail: tamas.gajda@chem.u-szeged.hu.
|| Universität des Saarlandes.
▽ E-mail: hegetschweiler@mx.uni-saarland.de.
⊥ Biocoordination Chemistry Research Group, University of Szeged.
ETH Hoenggerberg.

(1) Lipscomb, W. N.; Sträter, N. *Chem. Rev.* **1996**, *96*, 2375.
(2) For reviews on dinuclear functional models, see: (a) Chin, J. *Curr. Opin. Biol*. **1998**, *1*, 514. (b) Krämer, R.; Gajda, T. In *Perspectives in Bioinorganic Chemistry*; Hay, R. W., Dilwoth, J. R., Nolan, K., Eds.; JAI Press Inc.: Stamford, 1999; Vol. 4, pp 207−240.
(3) (a) Takasi, B. T.; Chin, J. *J. Am. Chem. Soc*. **1995**, *117*, 8582. (b) Oh, S. J.; Song, K. H.; Whang, D.; Kim, K.; Yoon, T. H.; Moon, H.; Park, J. W. *Inorg. Chem*. **1996**, *35*, 3780. (c) Hettich, R.; Schneider, H.-J. *J. Am. Chem. Soc*. **1997**, *119*, 5638. (d) Ott, R.; Krämer, R. *Angew. Chem., Int. Ed*. **1998**, *37*, 1957. (e) Bracken, K.; Moss, R. A.; Ragunathan, K. G. *J. Am. Chem. Soc*. **1997**, *119*, 9323. (f) Kim, A. D.; Burstyn, J. N. *Inorg. Chem*. **1996**, *35*, 2792. (g) Molenveld, P.; Engbersen, J. F. J.; Kooijman, H.; Spek, A. L.; Reinhoudt, D. N. *J. Am. Chem. Soc*. **1998**, *120*, 6726.
(4) (a) Morrow, J. N.; Aures, K.; Epstein, D. *J. Chem. Soc., Chem. Commun*. **1995**, 2431. (b) Koike, T.; Inoue, M.; Kimura, E.; Shiro, M. *J. Am. Chem. Soc*. **1996**, *118*, 3091. (c) Young M. J.; Wahnon D.; Hynes R. C.; Chin J. *J. Am. Chem. Soc*. **1995**, *117*, 9441.
(5) (a) Magda, D.; Wright, M.; Crofts, S.; Lin, A.; Sessler, J. L. *J. Am. Chem. Soc*. **1997**, *119*, 6947. (b) Matsumura, K.; Komiyama, M. *J. Biochem*. **1997**, *122*, 387. (c) Matsuda, S.; Ishikubo, A.; Kuzuya, A.; Yashiro M.; Komiyama, M. *Angew. Chem., Int. Ed*. **1998**, *37*, 3284.
(6) (a) Kövári, E.; Krämer, R. *J. Am. Chem. Soc*. **1996**, *118*, 12704. (b) Liu, S.; Hamilton, A. D. *Chem. Commun*. **1999**, 587. (c) Wall, M.; Linkletter, B.; Williams, D.; Lebuis, A.-M.; Hynes R. C.; Chin, J. *J. Am. Chem. Soc*. **1999**, *121*, 4710.
(7) Hegetschweiler, K. *Chem. Soc. Rev*. **1999**, *28*, 239.

10.1021/ic0005902 CCC: $20.00
Published on Web 08/07/2001

Table 1. Potentiometric Data (25 °C, $I = 0.1$ M KCl) of Cu(II)−tdci Systems[a]

Cu:tdci	1:4	1:2	1:1	2:1	3:1
$[Cu]_t$, mM	0.5	0.5	2.0, 1.0, 0.5	1.0	1.5
$[tdci]_t$, mM	2.0	1.0	2.0, 1.0, 0.5	0.5	0.5
no. of data points/ titration	110	100	90	100	110
time/point, min	10	10	10	10	10
pH range	4.3−10.0	4.4−10.2	4.4−10.4	4.5−11.1	4.5−10.5
no. of titrations	4	4	9	6	4

[a] Titrant: 0.1 M KOH.

in part due to their rather rigid, preorganized structures. Derivatization of the parent ligand taci (1,3,5-triamino-1,3,5-trideoxy-*cis*-inositol) also provides excellent possibilities for the design of tailored chelating agents which exert influence over the structure, stability, or electronic properties of the metal complexes. Due to the very strong intraligand repulsions, the dimethylamino groups of tdci are fixed in the equatorial positions and the three axial hydroxy groups provide selective binding sites for hard and highly charged metal ions.[8] Additionally, tdci offers also three facial $\{O_{ax},N_{eq},O_{ax}\}$ coordination sites,[9] which may be preferred by late transition metals such as copper(II). Our aim was to exploit this coordination to form alkoxo-bridged di- and trinuclear complexes, in which the metal ions are relatively close to each other, thereby allowing metal−metal cooperation in the binding and hydrolysis of phosphoesters. In the presence of a 2-fold excess of metal, the Cu^{II}−tdci system was, indeed, found to be a very efficient catalyst for the hydrolysis of the activated phosphodiester BNPP.

Several highly active copper(II) complexes have recently been reported to achieve the high hydrolytic efficiency of lanthanide ions.[6] The related Cu^{II}-*all-cis*-1,3,5-triaminocyclohexane system has also been shown to promote the efficient hydrolysis of phosphodiesters.[10] However, the presence of hydroxy groups in tdci leads to fundamental changes in the structure and composition of the formed complexes, and since the metal-bound alkoxo groups are, in many cases, more reactive nucleophiles in phosphoester hydrolysis than metal-bound hydroxide ions, this may lead to enhanced activity.[4]

Experimental Section

Physical Measurements. UV/vis spectra were measured on a Hewlett-Packard 8452A diode array spectrophotometer. The collection of pH-dependent series of spectra was performed by equipping a titration cell (50 mL solution, $[Cu^{II}] = 20$ mM, $I = 1$ M, $T = 25.0 \pm 0.1°$) with an immersion probe (HELLMA) connected to a diode array spectrophotometer (J&M, TIDAS-UV/NIR/100-1). This setting rendered the registration of the sample spectrum possible at any point of the potentiometric titrations. Continuous wave (CW) electron paramagnetic resonance (EPR) measurements were performed on a Bruker ESP300 spectrometer (microwave frequency 9.47 GHz) equipped with a liquid nitrogen cryostat and cooling equipment from Oxford and Cryogenics Inc. All measurements were carried out using 150 μL of 5 mM frozen solutions of 50% H_2O/50% DMSO. The spectra were measured with a modulation amplitude of 0.5 mT and a modulation frequency of 100 kHz. The pulse EPR and electron nuclear double resonance (ENDOR) experiments[11] were measured at X-band on a Bruker ESP380 spectrometer (microwave frequency 9.65 GHz). The HYSCORE experiment with the pulse sequence $\pi/2-\tau-\pi/2-t_1-\pi-t_2-\pi/2-\tau$-echo, measured at 20 K, used 16 ns $\pi/2$ pulses, a 16 ns transfer π pulse, and an eight-step phase cycle. In each of the two dimensions 512 data points were recorded at 16 ns intervals, with initial t_1 and t_2 values of 96 ns and a τ value of 102 ns. Two Davies-ENDOR experiments with the pulse sequence $\pi-T-\pi/2-\tau-\pi-\tau$-echo were measured at 20 K. One sequence used a 200 ns π pulse, and the second sequence used a 40 ns π pulse (hyperfine contrast selectivity to suppress weakly coupled protons). A radio frequency pulse with a length of 10 μs and a flip angle of π for the protons was used. The magnetization vs temperature and applied field was measured with a Cryogenics S600 SQUID magnetometer. The data were corrected for the diamagnetic contribution using Pascal's constants. FAB^+ mass spectra were measured on a VG ZAB-VSEQ instrument. The samples were dissolved in water and were mixed with a glycerol matrix prior to introduction into the spectrometer.

Potentiometric Measurements. The potentiometric titrations were carried out with a Metrohm 713 pH/mV meter and a combined glass electrode (Metrohm). The stability of the electrode was checked by a calibration titration prior to and after each measurement. The 50 mL sample solutions were titrated at 25.0 °C under nitrogen with 0.1 M (or 1 M) KOH, dispensed from a Metrohm 665 piston buret. The sample solutions were prepared from stock solutions of $CuCl_2$ and corresponding amounts of tdci·3HCl·$2H_2O$.[8] The ionic strength was adjusted to the desired value (0.1 or 1.0 M) by adding appropriate amounts of KCl or KNO_3, respectively, to the solutions. Detailed experimental data of the potentiometric measurements are given in Table 1.

Calculations of the Stability Constants. All equilibrium constants were calculated as concentration constants. The determination of the formation constants was performed with fixed pK_a's (5.93, 7.64, 9.68 at $I = 0.1$ M and 6.43, 8.12 and 9.96 at $I = 1$ M) obtained from several titrations of tdci·3HCl and fixed total concentrations of Cu^{II}, tdci, and H^+. In the case of the potentiometric measurements at $I = 0.1$ M, a consistent model was obtained using the computer program SUPERQUAD[12] while the combined potentiometric−photometric data at $I = 1$ M were evaluated by the program PSEQUAD.[13]

Preparation of $[Cu_5(tdciH_{-2})tdci_2(OH)_2(NO_3)_2](NO_3)_4\cdot 6H_2O$. tdci·3HCl·$2H_2O$[8] (300 mg; 0.74 mmol) was dissolved in 20 mL of H_2O and subjected to ion-exchange chromatography (DOWEX 2x8, OH^- form). A solution of $Cu(NO_3)_2\cdot 3H_2O$ (176 mg, 0.73 mmol) in H_2O (10 mL) was added, resulting a dark-blue solution. The solvent was removed under reduced pressure, and the resulting solid was dissolved in boiling EtOH/H_2O. On cooling to 4 °C both a green solid and a blue solid crystallized, which were filtered off. EtOH was added, and the green solid was redissolved by gentle heating. The green solution was decanted and allowed to cool slowly to room temperature. Green crystals, which proved to be suitable for single-crystal X-ray analysis, were obtained.

X-ray Diffraction Studies. The crystals of $[Cu_5(tdciH_{-2})(tdci)_2(OH)_2(NO_3)_2](NO_3)_4\cdot 6H_2O$ proved to be extremely unstable and disintegrated immediately after removal from their mother liquor. Furthermore, a first structure analysis at room temperature revealed a highly disordered structure. Therefore, a suitable crystal was embedded in a perfluoropolyether (RS3000, Riedel de Haen) and was immediately cooled to 200 K. Data collection was performed on a Stoe IPDS diffractometer

(8) Hegetschweiler, K.; Kradolfer, T.; Gramlich, V.; Hancock, R. D. *Chem. Eur. J.* **1995**, *1*, 74.
(9) Hedinger, R.; Ghisletta, M.; Hegetschweiler, K.; Tóth, E.; Merbach, A. E.; Sessoli, R.; Gatteschi, D.; Gramlich, V. *Inorg. Chem.* **1998**, *37*, 6698.
(10) (a) Itoh, T.; Hisada, H.; Sumiya, T.; Hosono, M.; Usui, Y.; Fujii, Y. *Chem. Commun*. **1997**, 677. (b) Itoh, T.; Hisada, H.; Usui, Y.; Fujii, Y. *Inorg. Chim. Acta* **1998**, *283*, 51.
(11) Schweiger, A.; Jeschke, G. *Principles of Pulse Electron Paramagnetic Resonance*; Oxford University Press: Oxford, 2001.
(12) Gans, P.; Sabatini, A.; Vacca, A. *J. Chem. Soc., Dalton Trans*. **1985**, 1195.
(13) Zékány, L.; Nagypál, I. PSEQUAD: A Comprehensive Program for the Evaluation of Potentiometric and/or Spectrophotometric Equilibrium Data Using Analytical Derivatives. In *Computational Methods for the Determination of Formation Constants*; Leggett, D. J., Ed.; Plenum Press: New York, 1991.

Table 2. Crystallographic Data for $[Cu_5(tdciH_{-2})(tdci)_2(OH)_2(NO_3)_2](NO_3)_4 \cdot 6H_2O$

empirical formula	$C_{36}H_{93}Cu_5N_{15}O_{35}$
fw (g/mol)	1613.95
cryst size, mm	0.2 × 0.15 × 0.1
cryst syst	triclinic
space group	$P\bar{1}$ (No. 2)
a, Å	11.551(2)
b, Å	12.542(3)
c, Å	26.657(5)
α, deg	93.14(3)
β, deg	95.30(3)
γ, deg	116.51(3)
V, Å^3	3421.0(12)
Z	2
T, °C	−73
λ, Å	0.70173 (Mo Kα)
ρ_{calcd}, g cm^{-3}	1.567
μ, cm^{-1}	16.25
R [$I > 2\sigma(I)$]	0.0843
wR2	0.2375

Table 3. Selected Bond Distances (Å) and Bond Angles (deg) of $[\mathbf{1}]^{4+}$ with Estimated Standard Deviations in Parentheses

Cu1−O7	1.923(7)	Cu1−O11	1.928(7)
Cu1−O10	1.970(7)	Cu1−N7	2.056(10)
Cu1−O20	2.538(14)	Cu2−O10	1.944(7)
Cu2−N3	2.010(9)	Cu2−O1	2.050(7)
Cu2−O30	2.087(11)	Cu2−O3	2.137(8)
Cu2−O31	2.474(12)	Cu3−O4	1.932(8)
Cu3−O11	1.940(8)	Cu3−O10	1.972(7)
Cu3−N4	2.026(9)	Cu3−O17b	2.688(17)
Cu4−O3	1.903(7)	Cu4−O4	1.952(8)
Cu4−N2	2.044(11)	Cu4−N6	2.090(10)
Cu5−O1	1.918(8)	Cu5−O7	1.980(8)
Cu5−N1	2.050(10)	Cu5−N9	2.090(9)
O7−Cu1−O10	91.7(3)	O30−Cu2−O3	104.3(3)
O11−Cu1−O10	81.3(3)	O4−Cu3−O10	92.6(3)
O7−Cu1−N7	86.8(3)	O11−Cu3−O10	80.9(3)
O11−Cu1−N7	100.1(4)	O4−Cu3−N4	85.8(3)
O11−Cu1−Cu3	41.2(2)	O11−Cu3−N4	101.0(4)
O10−Cu1−Cu3	42.3(2)	O11−Cu3−Cu1	40.9(2)
O10−Cu2−N3	164.9(4)	O10−Cu3−Cu1	42.3(2)
O10−Cu2−O1	90.3(3)	O3−Cu4−O4	89.7(3)
N3−Cu2−O1	83.1(3)	O3−Cu4−N2	86.7(4)
O10−Cu2−O30	93.4(4)	O4−Cu4−N6	82.7(4)
N3−Cu2−O30	98.3(4)	N2−Cu4−N6	102.8(4)
O1−Cu2−O30	155.4(4)	O1−Cu5−O7	93.3(3)
O10−Cu2−O3	86.9(3)	O1−Cu5−N1	85.1(3)
N3−Cu2−O3	81.0(4)	O7−Cu5−N9	82.9(4)
O1−Cu2−O3	100.3(3)	N1−Cu5−N9	100.7(4)

using Mo Kα radiation and a graphite monochromator. The data were corrected for Lorentz and polarization effects. The structure was solved by direct methods (SHELXS-97) and refined by full-matrix least-squares calculations on F^2 (SHELXL-97).[14,15] A summary of the crystallographic data is given in Table 2, and important bond lengths and bond angles of the complex core are listed in Table 3. The five Cu atoms and all the non-hydrogen atoms of the three tdci ligands could be located unambiguously. However, two of the six nitrate entities and one water molecule proved to be disordered. The disordered nitrate **(**which is coordinated to Cu1 and Cu3 in a bridging fashion**)** was modeled with one fully occupied oxygen position for one of the coordinated oxygen atoms and two partially occupied positions for the nitrogen and the remaining atoms. The second disordered nitrate exhibited no direct interaction with the complex. It was modeled with one position for the nitrogen and six positions for the three oxygen atoms, each with about 50% occupancy. All these partially occupied positions were refined isotropically. The other non-hydrogen atoms were refined with anisotropic displacement parameters. The structure was not of sufficient quality to locate hydrogen atoms unambiguously. Therefore, the H(−C) positions were calculated using a riding model and constant isotropic displacement parameters of 0.08 Å^2. Other hydrogen atomic positions (O−H or N−H) were not considered.

(14) Sheldrick, G. M. *SHELXS-97: Program for the solution of crystal structures*; University of Göttingen: Göttingen, Germany, 1997.

(15) Sheldrick, G. M. *SHELXL-97, Program for refinement of X-ray structures*; University of Göttingen: Göttingen, Germany, 1997.

Table 4. Formation Constants of Cu^{II}−tdci Complexes at Two Different Ionic Strengths ($T = 298$ K) with Estimated Standard Deviations in Parentheses[a]

	log *β*	
	$I = 0.1$ M	$I = 1.0$ M
$Cu(tdci)H_{-1}$	1.74(8)	
Cu(tdci)	9.4(1)	11.0(2)
Cu(tdci)H	15.23(7)	16.2(2)
$Cu_2(tdci)H_{-6}$	−37.35(9)	
$Cu_2(tdci)H_{-5}$	−26.06(4)	−25.8(2)
$Cu_2(tdci)H_{-4}$	−15.2(1)	−13.44(6)
$Cu_2(tdci)H_{-3}$	−5.9(1)	−3.84(6)
$Cu_2(tdci)H_{-2}$	1.52(5)	2.7(1)
$Cu_2(tdci)H_{-1}$	7.51(4)	8.52(6)
$Cu_2(tdci)$	12.9(1)	13.2(2)
$Cu_3(tdci)H_{-6}$	−24.21(3)	−22.7(1)
$Cu_3(tdci)H_{-5}$	−14.4(1)	−12.77(5)
$Cu_3(tdci)H_{-4}$	−7.25(1)	−5.97(3)
$Cu_3(tdci)H_{-3}$	−1.1(2)	−0.9(2)

[a] $\beta(Cu_x(tdci)H_{-y}) = [Cu_x(tdci)H_{-y}] \times [Cu]^{-x} \times [tdci]^{-1} \times [H]^y$.

Kinetic Measurements. The hydrolysis of BNPP and DNPEP[16] was followed by spectrophotometry, detecting the formation of the corresponding (di)nitrophenolate anion (ϵ(400 nm) = 18900, pK = 6.98 and 4.02, respectively) in aqueous solution at $I = 0.1$ M and $T = 298$ K. The reported kinetic data, determined by both initial slope (≤4% conversion) and integral methods (∼ 90% conversion), are averages of triplicate measurements (reproducibility better than 10%). The initial concentration of the substrates varied from 0.02 mM to 5 mM (BNPP) and 18 mM (DNPEP). In all cases 0.02 M buffer (HEPES and CHES) was used. In a typical experiment, the pH of the solution containing 0.5 mM tdci and 1 mM copper(II) was adjusted to the desired value. After 5 min equilibration, 100 *μ*L of 0.02 M BNPP (20 *μ*L 0.002 M in the case of integral measurements) was injected into the solution with efficient mixing. The increase of the absorbance at 400 nm was followed. Second-order rate constants were obtained from plots of first-order rate constants against the concentration of Cu_2LH_{-3} species, calculated from the formation constants given in Table 4.

Results and Discussion

The Crystal Structure and Magnetic Properties of $[Cu_5(tdciH_{-2})tdci_2(OH)_2(NO_3)_2](NO_3)_4 \cdot 6H_2O$ ($[\mathbf{1}](NO_3)_4 \cdot 6H_2O$). Unfortunately, crystals of this compound proved to be of very low stability. Rapid disintegration **(**which was probably due to loss of water**)** was observed in air. Several attempts were made to collect an appropriate data set; however, due to the low stability of the crystals and the disorder problem (encountered with two NO_3^- ions and one H_2O molecule), the structure solution was not completely satisfactory. Nonetheless, the structure is of sufficient quality to discuss the coordination geometry of the five Cu^{II} centers and the connectivity within the complex $[\mathbf{1}]^{4+}$ (Figure 1). The low stability of the crystal packing is probably caused by the nine bulky dimethylamino groups of the three ligand entities, which generate a rather lipophilic molecular surface and largely prevent the formation of a stabilizing hydrogen-bonding network. Although hydrogen atomic positions could not be located unambiguously, the assumption that (i) a bridging oxygen atom within the ligand must be interpreted as a μ_2-alkoxo rather than a μ_2-hydroxo bridge and (ii) terminally coordinating oxygen atoms of the ligand with a Cu−O distance longer than 2.3 Å (Table 3) must

(16) Moss, R. A.; Ihara, Y. *J. Org. Chem.* **1983**, *48*, 588.

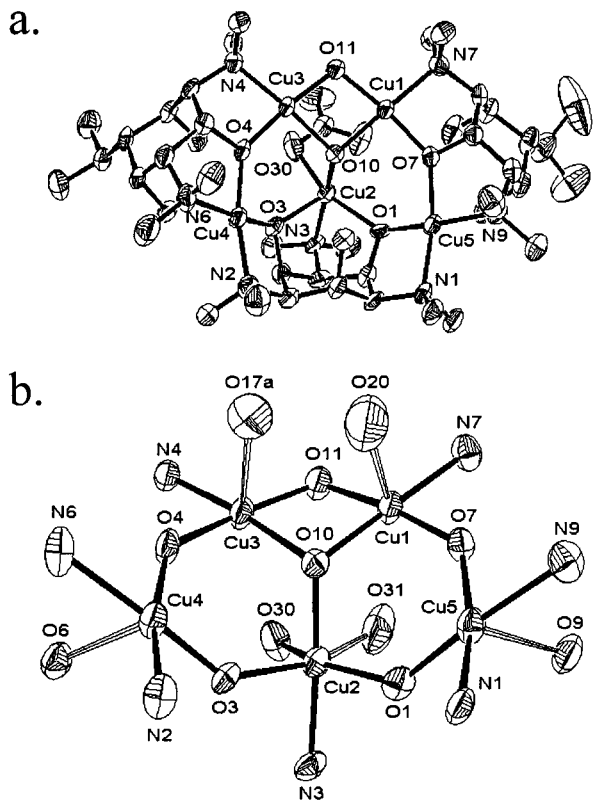

Figure 1. (a) ORTEP view (50% probability) of $[\mathbf{1}]^{4+}$ with atom-labeling scheme. Hydrogen atoms, nitrate ions (except for $N(13)O_3^-$), and water molecules are omitted for clarity. (b) Part of the structure of $[\mathbf{1}]^{4+}$, emphasizing the coordination environments of the copper(II) ions and the Cu_5O_6 core.

be interpreted as coordinated hydroxy groups, together with consideration of the charge balance**,** resulted in an unambiguous assignment of the structure. The pentanuclear complex $[\mathbf{1}]^{4+}$ is built up from two dinuclear units and one trinuclear unit, having two shared copper(II) ions (Cu4 and Cu5**)**. The five Cu^{II} centers in the complex exhibit three distinct types of coordination geometries. Cu1 and Cu3 have a "4 + 1" type square pyramidal $\{NO_3 + O\}$ coordination with two hydroxo groups, an alkoxo group, and a loosely bound, apical nitrate oxygen. The two metal centers are linked by a μ-dihydroxo bridge (O10 and O11) and by two oxygens of the disordered N17 nitrogen group. The main difference between the two copper(II) ions is the apical bond lengths **(**2.54 and 2.70 Å for Cu1 and Cu3, respectively**)**. The Cu4 and Cu5 ions have a similar "4 + 1" square pyramidal geometry, but with $\{N_2O_2 + O\}$ coordination. Two amino nitrogens and two alkoxo oxygens occupy the basal positions while non-deprotonated hydroxy groups are coordinated in the apical sites. The Cu2 ion has strongly distorted octahedral geometry with an unusual $\{NO_4 + O\}$ coordination. The two axial positions are occupied by a loosely bound nitrate oxygen (O31) and by an alkoxo group (O3) having a relatively short Cu−O distance (Cu2−O3 = 2.137 Å). In the equatorial plane of Cu2 the N3 nitrogen, an alkoxo (O1), a hydroxo (O10), and a nitrate (O30) oxygen are coordinated. In this way, the Cu2 ion is chelated by a nitrate ion in a η^2-anisobidentate manner (the difference between the two $Cu2-O_{nitrate}$ distances is 2.47−2.09 = 0.39 Å, which is much less than the suggested cutoff for bidentate coordination[17]). The η^2-type binding of the nitrate ion imposes a small O30−Cu2−O31 angle (54.9°), which results in a substantial distortion of all other angles from ideal octahedral geometry.

In complex $[\mathbf{1}]^{4+}$, the equatorial Cu−O bond distances lie in the range 1.903(7)−1.980(8) Å (average 1.942 Å) except for the Cu2−O1 and Cu2−O30 bonds, which are 2.050(7) and 2.087(11) Å, respectively. These deviations are probably due to the constraints imposed by the aforementioned strongly distorted geometry of the Cu2 ion. The axial Cu−O bond distances are between 2.380 and 2.709 Å (with the exception of Cu2−O3). All nitrogens are coordinated in the basal planes of the central ions with Cu−N distances between 2.010 and 2.090 Å.

A remarkable feature of the structure is that Cu1, Cu2, and Cu3 are μ_3-bridged by a common hydroxide ion. In addition, another hydroxide and several alkoxo groups form μ_2-bridges between the copper(II) ions. As a result of this extensive O-bridging network, a unique Cu_5O_6 cage is formed within the complex $[\mathbf{1}]^{4+}$ (Figure 1b), displaying three distinct Cu−Cu distances. The μ-dihydroxo-bridged Cu1 and Cu3 ions are separated by 2.916(2) Å with Cu−O−Cu angles of 95.5° and 97.9°. Because of the constraints caused by the fused five-membered chelate rings of the ligand backbone, both the Cu−Cu distances and Cu−O−Cu angles in the alkoxo-bridged units are higher (3.627(2)−3.782(3) Å and 136−138.7°, respectively). These values are within the range observed for similar μ-dihydroxo-bridged[18] and μ-alkoxo-bridged[19] dinuclear copper(II) complexes. The Cu−Cu separations between the nonbridged metal ions are 5.455(3)−5.712(3) Å.

Another noteworthy characteristic of complex $[\mathbf{1}]^{4+}$ is the nonplanarity of the tetragonal planes of the bridged copper(II) ions. The least-squares planes Cu1 and Cu3 are tilted toward each other by 19°. Consequently, the Cu_2O_2 unit is not coplanar either, giving rise to a Cu1−O10−Cu3−O11 dihedral angle of 15.7(4)°. The basal planes of the monobridged centers are also considerably twisted. For example, the angles between the ls planes of Cu1/Cu5 and Cu3/Cu4 are 31.5(5)° and 38.9(5)°, respectively.

Although hydrogen atoms could not be located, there is some evidence that the two nitrogen atoms N5 and N8 are protonated. Both atoms have rather short contacts to the oxygen atoms of a nitrate counterion (2.75 Å) or to a water molecule (2.61 Å), respectively, which is indicative of N−H···O hydrogen bonding. The assignment of a positive charge on these two atoms is also required by the charge balance. Consequently, amino groups not involved in metal binding remain protonated, despite the presence of six hydroxo and alkoxo groups in the molecule.

The magnetic properties of the pentanuclear complex have been investigated in the 2−300 K temperature range. The room temperature value of the $\chi_M T$ product (1.09 emu K mol^{-1}) is considerably lower than expected for five uncoupled $S = {}^1/_2$ spins. The presence of strong antiferromagnetic interactions is also confirmed by the rapid decrease of $\chi_M T$ with decreasing temperature (Figure 2). Below 90 K, $\chi_M T$ is almost constant and close to the value expected for a spin $S = {}^1/_2$ with $g \approx 2.1$. The magnetization measured at 2.5 and 5.0 K lies almost on

(17) Kleywegt, G. J.; Wiesmeijer, W. G. R.; Van Driel, G. J.; Driessen, W. L.; Reedijk, J.; Noordik, J. H. *J. Chem. Soc., Dalton Trans*. **1985**, 2177.

(18) See, for example: Lewis, D. L.; Hatfield, W. E.; Hodgson, D. J. *Inorg. Chem*. **1972**, *11*, 2216.

(19) (a) Gajda, T.; Krämer, R.; Jancsó, A. *Eur. J. Inorg. Chem*. **2000**, 1635. (b) Satcher, J. H., Jr.; Droege, M. W.; Weakley, T. J. R.; Taylor, R. T. *Inorg. Chem*. **1995**, *34*, 3317. (c) Nie, H.; Aubin, S. M. J.; Mashuta, M. S.; Porter, R. A.; Richardson, J. F.; Hendrickson, D. N.; Buchanan R. M. *Inorg. Chem.* **1996**, *35*, 3325. (d) Frey, S. T.; Murthy, N. M.; Weintraub, S. T.; Thompson, L. K.; Karlin, K. D. *Inorg. Chem*. **1997**, *36*, 956.

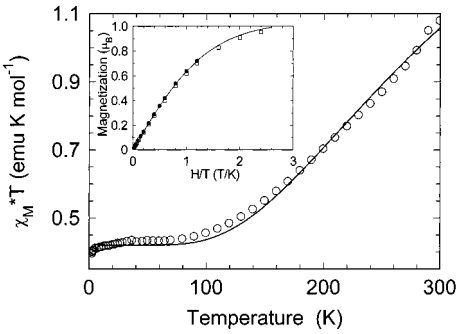

Figure 2. Plot of $\chi_M T/Cu^{II}_5$ vs T for a polycrystalline sample of [**1**]-$(NO_3)_4 \cdot 6H_2O$. The solid line represents the fit according to a simple theoretical model detailed in the text.

the same curve and is well reproduced by a Brillouin curve for $S = {}^1/_2$ and $g = 2.09$ (see the insert of Figure 2), confirming that only a single spin state is populated at low temperature.

The exchange interaction mediated by hydroxo/alkoxo bridges has been extensively studied and found to be strongly correlated to the Cu−O−Cu angle.[20] The exchange interaction is expected to vanish around 96−98° and to increase dramatically for increasing angles. In the present complex the lack of strict coplanarity of the $d_{x^2-y^2}$ orbitals of the bridged metal centers does not allow a quantitative estimation of the exchange interaction, but we can anticipate a strong antiferromagnetic interaction between Cu4−Cu3 and Cu5−Cu1 (Cu−O−Cu angles around 138°). A much weaker interaction is expected for the pair Cu1−Cu3 (Cu−O−Cu angles in the range 95.4−97.9°) as well as for the pairs Cu2−Cu1 and Cu2−Cu3. The assignment is more complex for the pairs Cu2−Cu4 and Cu2−Cu5 being strongly asymmetric. In fact, for the pair Cu2−Cu4/Cu5 the largest overlap is within the doubly filled d_{z^2} orbital of Cu2 and the $d_{x^2-y^2}$ magnetic orbital of Cu4/Cu5, leading to a ferromagnetic transition.

The experimental data, however, do not allow the quantitative evaluation of these different exchange interactions as the antiferromagnetic interactions strongly dominate over the others. The $\chi_M T$ curve in Figure 2 is indeed satisfactorily reproduced with our simple model, taking into account the contribution of two pairs of antiferromagnetically interacting spins (Cu1−Cu5, Cu3−Cu4) and an isolated $S = {}^1/_2$ spin (Cu2), using the Bleaney−Bowers formula with $J = 600$ cm^{-1} and $g = 2.10$ for the interacting spins and $g = 2.10$ for the isolated spin (solid curve in Figure 2). In the absence of additional data, e.g., single-crystal EPR spectra, the use of a more complex spin Hamiltonian with different J values could only lead to an overparametrization of the problem.

Equilibrium Study. The solution equilibrium behavior of Cu^{II} complexes of tdci has been already published,[21] but further studies indicated more complicated complex formation processes above pH 6, since no precipitation was observed up to 3-fold metal ion excess. These observations forced us to reinvestigate the solution speciation of the copper(II)−tdci system. The equilibrium properties of this system proved to be extremely complicated, and a very detailed pH-metric study has therefore been performed, including 27 independent titrations with a wide range of total Cu to total tdci ratios **(**ranging from 1:4 to 3:1**)**. These data can be consistently interpreted only by the coexistence of mono-, di-, and trinuclear species having different

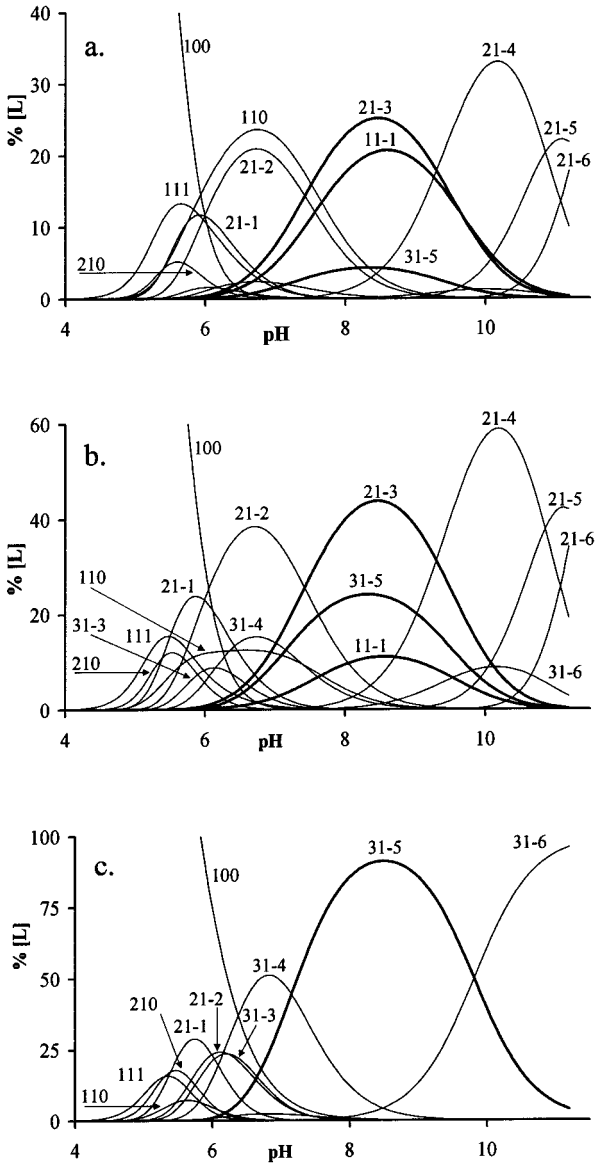

Figure 3. Species distribution curves in the Cu(II)−tdci system at different metal-to-ligand ratios (the percentage of the Cu_2LH_{-3} species is shown in bold); [Cu]:[L] = 1:1 (a), 2:1 (b), and 3:1 (c), [L] = 4.4×10^{-4} M, $T = 298$ K, $I = 0.1$ M (KCl). The different species $Cu_xL_yH_z$ are labelled as *xyz*.

degrees of protonation. The complex formation constants are listed in Table 4.

The formation of the Cu(II)−tdci complexes starts around pH 4−5 (Figure 3). The mononuclear complexes (CuLH, CuL, and $CuLH_{-1}$) are dominant only at 1:4 and 1:2 metal-to-ligand ratios below pH 9.5. On the other hand, polynuclear complexes (Cu_nLH_{-x}, $n = 2,3$, $x = 0-6$) exist even in the case of 4-fold ligand excess and always become dominant above pH 9.5. In equimolar solution or in the case of 2-fold metal excess, the dinuclear complexes are the major species in the entire pH range. At a 3:1 metal-to-ligand ratio, trinuclear species (Cu_3LH_{-x}, $x = 3-6$) are dominant above pH 6 (Figure 3c).

The question of the structure of these species therefore arises. Basically, the ligand provides four tridentate coordination sites for the metal ions: one $\{O_{ax},O_{ax},O_{ax}\}$ and three $\{O_{ax},N_{eq},O_{ax}\}$.[7] The O-donors of tdci may coordinate as either hydroxy or alkoxo groups. Other coordination modes, e.g., involving several nitrogen donors, would require ring inversion (e.g., chair

(20) (a) Crawford, V. H.; Richardson, H. W.; Wasson, J. R.; Hodgson, D. J.; Hatfield, W. E. *Inorg. Chem.* **1976**, *15*, 2107. (b) Merz, L.; Haase W. *J. Chem. Soc., Dalton Trans*. **1980**, 875.
(21) Kradolfer, T.; Hegetschweiler, K. *Helv. Chim. Acta* **1992**, *75*, 2243.

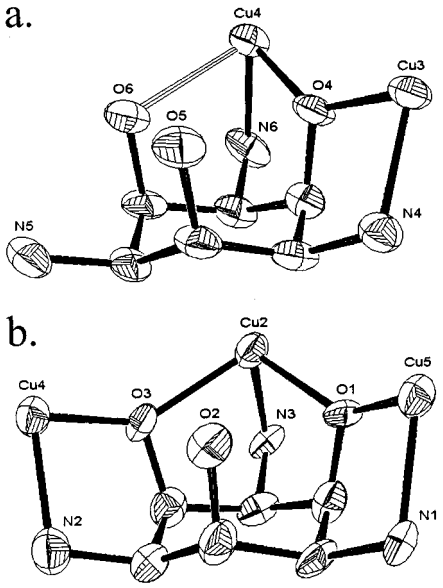

Figure 4. Alkoxo-bridged dinuclear and trinuclear fragments of $[\mathbf{1}]^{4+}$.

conformation), which is highly unfavored due to the strong intraligand repulsion between the dimethylamino groups.

On the basis of our X-ray study, a given ligand molecule in complex $[\mathbf{1}]^{4+}$ offers, indeed, bidentate $\{N_{eq},O^-_{ax}\}$ or tridentate $\{O^-_{ax},N_{eq},OH/O^-_{ax}\}$ side-on coordination to the metal ions. The alkoxo groups form bridges between two copper(II) ions coordinated to two adjacent amino nitrogens. No species related to complex $[\mathbf{1}]^{4+}$ (i.e., $[Cu_5L_3H_{-4}]^{4+}$) was found in solution. The structurally characterized pentanuclear complex is most likely formed by the aggregation of the species existing in neutral solution. Nevertheless, the single-crystal structure of $[\mathbf{1}]^{4+}$ may provide insight into the structures of the complexes that exist in solution. Figure 4 shows a dinuclear and a trinuclear segment of complex $[\mathbf{1}]^{4+}$, indicating the side-on coordination of metal ions.

When two or three $\{O_{ax},N_{eq},O_{ax}\}$ sites are occupied by metal ions, the O-donors of the ligand may serve as bridging units between two metal ions. Additionally, deprotonation of the metal-bound water molecules may occur. Taking into account the rather large Cu−Cu separation offered by tdci and the position of the (bridging) hydroxy/alkoxo groups, the metal-bound hydroxide ions are probably not able to form a bridge between two metal ions, i.e., they should adopt terminal coordination.

The pH-metric studies provide additional valuable information for the structural assignment of the solution species. The equilibrium constants (K_{Cu}) for the general process

$$Cu_xLH_{-y} + Cu = Cu_{x+1}LH_{-y} \qquad (K_{Cu})$$

increase for the complexes formed with successive deprotonation. The log K_{Cu} values of the above process are 3.50 and 5.77 in the case of CuL ($x = 1$, $y = 0$) and $CuLH_{-1}$ ($x = 1$, $y = 1$), respectively. Starting from dinuclear complexes ($x = 2$) the log K_{Cu} values are as follows: 4.90 ($y = 3$), 7.95 ($y = 4$) and 11.66 ($y = 5$). These values indicate considerably increasing metal-binding ability for successively formed complexes; i.e., during the stepwise deprotonations, the available binding sites become increasingly favored by the metal ions (the charge neutralization alone cannot be responsible for such additional stabilization). Accordingly, the above-mentioned log K_{Cu} values for, e.g., the dinuclear complexes reflect the copper(II) binding ability of a {OH,N,OH}, {OH,N,O$^-$}, and {O$^-$,N,O$^-$} donor set, respectively. Copper(II)-promoted deprotonation of hydroxy groups, at neutral or even lower pH, have been already described for several ligands where suitable anchoring donors are present.[23] In the case of tdci this process should be especially favorable, as a result of its preorganized structure.

The change in the speciation with increasing metal-to-ligand ratio at pH 8.6 was also followed by UV−vis spectrophotometry (Figure S1, Supporting Information). A significant red shift (70−80 nm) of the d−d band was observed as the [Cu]:[L] ratio changed from 1:4 to 3:1, probably due to the increasing distortion of the tetragonal symmetry caused by the stepwise formation of the triply bridged Cu_3LH_{-5} species with *facial* coordination of tdci. In addition, an intense LMCT band developed around 350 nm (Figure S1, inset), with the gradual formation of oligonuclear complexes, a characteristic feature of the alkoxo-bridged copper(II) centers.[23]

In order to verify the above-mentioned speciation, a combined pH-metric−spectrophotomeric solution equilibrium study has been performed. However, this required the use of a higher metal concentration (20 mM instead of 0.5−2 mM) and consequently a higher ionic strenght (1 M). The evaluation of these data indicated the formation of identical complexes at $I = 0.1$ and 1 M. Similarly, the determined formation constants (Table 4) agree well with each other, taking into account the different ionic strengths. The pH-dependent vis spectra of the Cu^{II}−tdci systems are depicted in Figure S2 (see Supporting Information). Between pH 5 and 7, there are a number of minor species; therefore, the photometric data can be correctly evaluated only above pH 7, where major species are formed and their speciations are well separated. The invidual visible spectra of the species Cu_2LH_{-3}, Cu_2LH_{-4}, Cu_2LH_{-5}, Cu_3LH_{-4}, Cu_3LH_{-5}, and Cu_3LH_{-6} (Figure S3, Supporting Information) are rather similar; their maximums are between 690 and 725 nm, according to the proposed $\{NO_x\}$ ($2 \le x \le 5$) coordination environment.[24]

The formation of a series of trinuclear species $[Cu_3(tdciH_{-x})(NO_3)(H_2O)_4]^+$ ($x = 1-3$) could also be observed in the FAB+ mass spectra: $[Cu_3(tdciH_{-3})(NO_3)(H_2O)_4]^+$ $m/z = 583.3$ (intensity 8.2%), $[Cu_3(tdciH_{-2})(NO_3)(H_2O)_4]^+$ 584.3 (12.6%), $[Cu_3(tdciH_{-1})(NO_3)(H_2O)_4]^+$ 585.4 (15.4%). The observed isotopic and intensity pattern could be well reproduced by overlaying the three above-mentioned species.

A CW and pulse EPR study was performed to obtain further structural information on the mononuclear, dinuclear, and trinuclear complexes. Figure 5 shows CW spectra of frozen solutions containing (a) predominately mononuclear complexes; (b−d) predominately dinuclear complexes with 0%, 10%, and 50% Zn substitution, respectively; and (e−g) trinuclear complexes measured at 150, 10, and 4.3 K respectively. The mononuclear complexes (Figure 5a) have an axial spectrum typical for square-planar or elongated octahedral geometry, with g values of $g_{\|} \approx 2.244$ and $g_{\perp} \approx 2.050$ and copper hyperfine couplings of $|A_{\|}| \approx 555$ MHz and $|A_{\perp}| \approx 75$ MHz. These values are only approximate since the spectrum is a superposition of the spectra of three different mononuclear complexes having slightly different parameters. Traces b−d are plotted with quantitative relative intensities, with trace b being ≈15% as intense as that of the mononuclear complexes in trace a. We attribute spectrum b to small concentrations of mononuclear and

(22) Hedinger, R.; Kradolfer, T.; Hegetschweiler, K.; Wörle, M.; Dahmen, K.-H. *Chem. Vap. Deposition* **1999**, *5*, 29.
(23) (a) Gyurcsik, B.; Gajda, T.; Jancsó, A.; Lammers R.; Nagy, L. *J. Chem. Soc., Dalton. Trans.* **1997**, 2125. (b) Gajda, T.; Gyurcsik, B.; Jakusch, T.; Burger, K.; Henry, B.; Delpuech, J.-J. *Inorg. Chim. Acta* **1998**, *275−276*, 130.
(24) Sigel, H.; Martin, R. B. *Chem. Rev.* **1982**, *82*, 385.

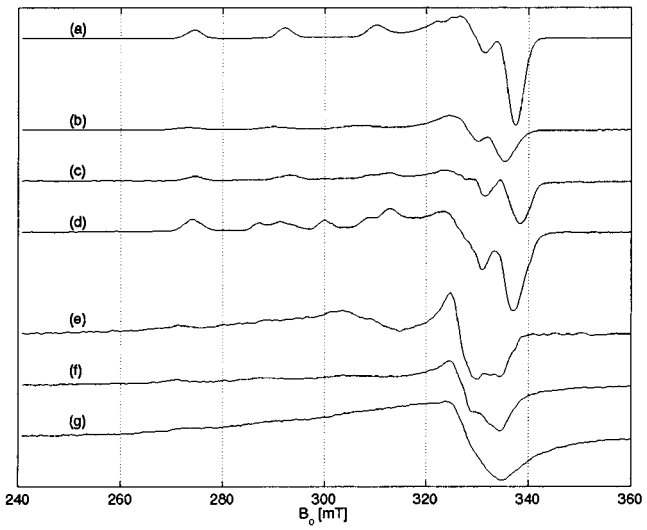

Figure 5. CW EPR spectra, measured at 150 K, of (a) mononuclear complexes of 1:4 Cu(II):tdci at pH 6.5, (b−d) dinuclear complexes of 1:1 Cu(II):tdci at pH 11 with 0%, 10%, and 50% Zn substitution, respectively, and (e−g) trinuclear complexes of 3:1 Cu(II):tdci at pH 10.5 measured at a temperature of 150, 10, and 4.3 K, respectively.

possibly trinuclear species, since the dinuclear complexes are EPR silent (see below). Addition of Zn^{II} resulted in a clear increase in signal intensity, with the 10% Zn (c) and 50% Zn (d) samples being ≈25% and ≈50% as intense as the spectrum of the mononuclear complexes in trace a. We attribute this increase in signal intensity to the formation of mixed dinuclear complexes containing one paramagnetic Cu^{II} ion and one diamagnetic Zn^{II} ion. These data confirm the existence of dinuclear copper(II) complexes being EPR silent (from 298 to 10 K), a result consistent with strong antiferromagnetic coupling between the copper(II) ions.[25] We were not able to quantitatively analyze the data, presumably because the frozen solutions contain several different dinuclear and small quantities of mononuclear and trinuclear complexes. However, the increase in signal intensity by substituting Cu^{II} ions with Zn^{II} ions is evident.

The spectra of the trinuclear complexes, traces e−g in Figure 5, have *g* values and copper hyperfine couplings which differ from those of the mononuclear complexes and vary as a function of temperature (see also Figure S4 in the Supporting Information). Such behavior has also been observed before for trinuclear complexes and was attributed to variations in the thermal population of doublet and quadruplet spin states.[26] Our spectra might be interpreted as consisting of a superposition of spectra from two spin states, presumably the two doublet states, with the higher energy state being depopulated at 4.3 K.

ENDOR measurements provided valuable information about the coordination sphere of the mononuclear copper(II) complexes. Figure 6 shows two X-band ENDOR spectra recorded at a field position of 307 mT (see trace a in Figure 5). Hyperfine contrast selective ENDOR was used to attenuate the spectrum of the weakly coupled ^1H nuclei which in this case overlaps with the spectrum of a strongly coupled ^{14}N nucleus with A ∼27−28 MHz. In Figure 6b, where short microwave pulses

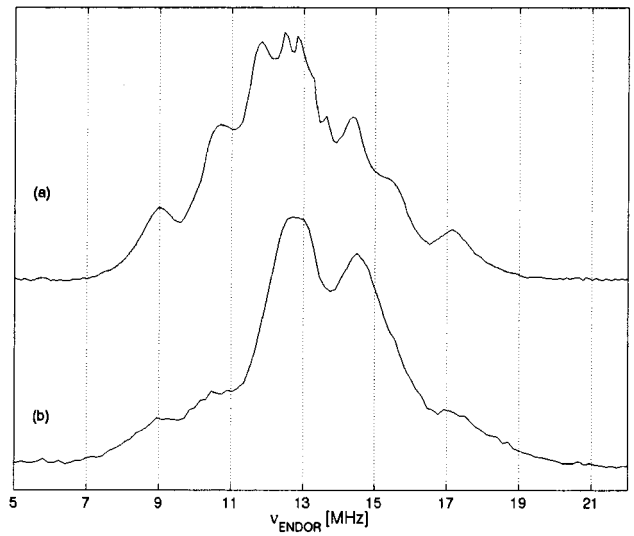

Figure 6. Hyperfine contrast selective Davies-ENDOR spectra at X-band and $B_0 = 307$ mT of the mononuclear complexes. Trace a uses a π pulse of length 200 ns; trace b uses a π pulse of length 20 ns to suppress the weak ^1H couplings. The spectrum of the weakly coupled ^1H nuclei is centered around the Larmor frequency, $\nu_H = 13.1$ MHz, whereas the spectrum of the strongly coupled ^{14}N is centered at half its hyperfine coupling, $A/2 = 13.7$ MHz, split by $2\nu_N = 1.9$ MHz.

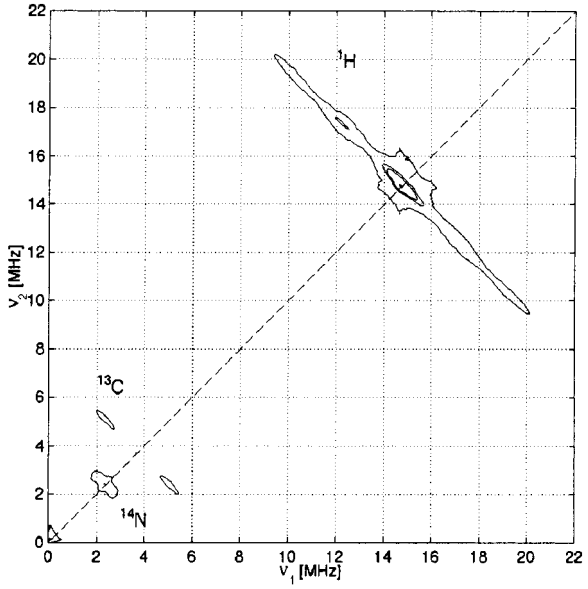

Figure 7. X-band HYSCORE spectrum measured at $B_0 = 347$ mT; couplings from ^1H, ^{13}C, and ^{14}N nuclei are indicated.

were used to suppress the ^1H signals, interactions from at least one strongly coupled ^{14}N nucleus are visible. These results were confirmed by Q-band Davies-ENDOR measurements where ^1H and ^{14}N interactions are well separated owing to the much higher resonance frequencies of the protons (see Figures S5 and S6 in the Supporting Information). Since there is a strongly coupled nitrogen, it can be concluded that one lobe of the $d_{x^2-y^2}$ copper orbital containing the unpaired electron points at the nitrogen. In order to detect additional weak hyperfine couplings, a HYSCORE experiment was performed (Figure 7). The HYSCORE spectrum shows ^1H hyperfine couplings up to ∼10 MHz, which are characteristic for water coordinated to a Cu^{II} ion.[27] In addition, hyperfine couplings of ^{13}C in natural abundance (A ∼2−3.4 MHz) and double-quantum peaks from

(25) See, for example: Torelli, S.; Belle, C.; Gautier-Luneau, I.; Pierre, J. L.; Saint-Aman, E.; Latour, J. M.; Le Pape, L.; Luneau, D. *Inorg. Chem.* **2000**, *39*, 3526. (b) Bencini, A.; Gatteschi, D. *EPR of Exchanged Coupled Systems*; Springer-Verlag: Berlin, 1990.

(26) (a) Gutierrez, L.; Alzuet, G.; Real, J. A.; Cano, J.; Borras, J.; Castineiras, A. *Inorg. Chem.* **2000**, *39*, 3608. (b) Banci, L.; Bencini, A.; Gatteschi, D. *Inorg. Chem.* **1983**, *22*, 2681.

(27) Atherton, N. M.; Horsewill, A. J. *Mol. Phys.* **1979**, *5*, 1349.

Chart 1[a]

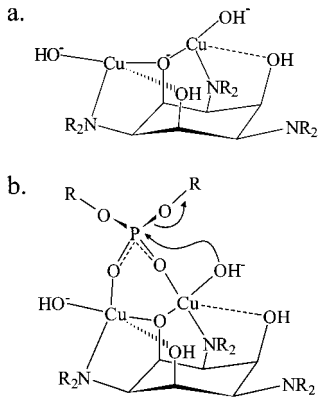

[a] Proposed structure of the Cu_2LH_{-3} species (additional water molecules bound to the metal ions are possible). [b] Proposed mechanism of BNPP hydrolysis by the Cu_2LH_{-3} species.

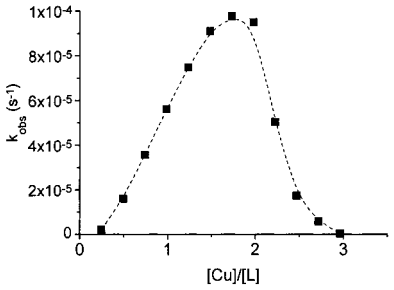

Figure 8. Dependence of the rate of BNPP hydrolysis on the $[Cu^{II}]$:[tdci] ratio at constant ligand concentration; pH = 8.60, [tdci] = 4.6×10^{-4} M, $T = 298$ K.

very weakly coupled ^{14}N nuclei can be observed. These latter cross peaks indicate that nitrogen nuclei remote from the copper(II) ion (>6 Å) are also present in the mononuclear complexes.

The pulse EPR data are in favor of the side-on $\{O_{ax},N_{eq},O_{ax}\}$ type coordination of copper(II) in CuL. This explains the formation of di- and trinuclear complexes, since three identical $\{O_{ax},N_{eq},O_{ax}\}$ binding sites are available in tdci. Closely related trinuclear alkoxo-bridged structures were found in several metal complexes of the nonmethylated ligand taci[8] and in a trinuclear Pb^{II} complex of tdci.[22]

In conclusion, the structure depicted in Chart 1a can be proposed for the Cu_2LH_{-3} species. It is not possible to rule out the deprotonation of the adjacent hydroxy groups instead of the coordinated water molecules, although some of the hydrolytic measurements (see below) also suggest deprotonation of water ligands.

Kinetic Study. To screen the phosphoesterase activity of the copper(II)−tdci system, the hydrolysis of the activated phosphodiester BNPP was followed. In light of the formation of mono-, di-, and trinuclear species in different protonation states, the BNPP hydrolysis promoted by the copper(II)−tdci system is expected to be strongly dependent on the metal-to-ligand ratio and pH. Indeed, bell-shaped curves have been obtained for the pseudo-first-order rate constants when either of these parameters was varied. The dependence on the metal-to-ligand ratio (Figure 8) indicates that the maximum activity is reached at a 2-fold excess of metal, while the pH−rate profile at a 2:1 metal-to-ligand ratio (Figure 9) shows a maximum around pH = 8.6.

In the pH range 7.5−9.5, three complexes predominate, namely, $CuLH_{-1}$, Cu_2LH_{-3}, and Cu_3LH_{-5}, depending on the metal-to-ligand ratio. Since at [Cu]:[L] = 3:1 no hydrolytic activity was detected, the trinuclear complex is inactive, as is

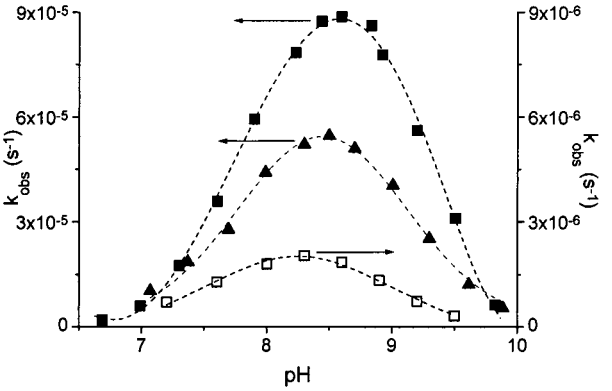

Figure 9. The pH−rate profile of BNPP, DNPEP, and NPP hydrolysis promoted by the Cu^{II}−tdci system. ■: $[Cu^{II}] = 2[L] = 8.80 \times 10^{-4}$ M, [BNPP] = 1×10^{-3} M, $T = 298$ K. ▲: $[Cu^{II}] = 2[L] = 8.85 \times 10^{-4}$ M, [DNPEP] = 1×10^{-3} M, $T = 298$ K. □: $[Cu^{II}] = 2[L] = 3 \times 10^{-3}$ M, [NPP] = 3×10^{-3} M, $T = 298$ K.

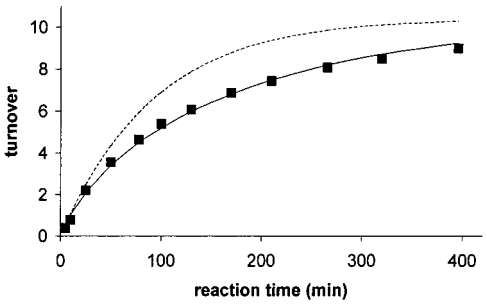

Figure 10. Catalyzed hydrolysis of BNPP using 10.5-fold excess of substrate over the dinuclear Cu_2LH_{-3} complex; pH = 8.60, $[Cu_2LH_{-3}] = 2.55 \times 10^{-4}$ M. The dotted line shows the ideal behavior; the solid line was calculated using $K = 490$ M^{-1} for formation of the inactive mixed-ligand complex ($Cu_2LH_{-3}^{+} + NPP^{2-} = [Cu_2LH_{-3}(NPP)]^{-}$).

the free ligand tdci. On the other hand, the increasing hydrolytic activity between [Cu]:[L] = 1:4 and 2:1 is paralleled by the increasing concentration of the Cu_2LH_{-3} species. Consequently, the observed hydrolytic activity can be attributed to the dinuclear complex, while the hydrolysis promoted by the mononuclear complex is negligible. On the basis of the pH−rate profile, the activity of other species formed at lower or higher pH can be also neglected, since the bell-shaped curve in Figure 9 is even somewhat narrower than the distribution curve of Cu_2LH_{-3}. This is probably due to the slight change of equilibria induced by the presence of BNPP and buffers used in the kinetic study.

Separate experiments established that the copper(II)−tdci system also promotes the hydrolysis of the product NPP. The bell-shaped pH−rate profile of NPP hydrolysis was found to be nearly identical with that of the BNPP (Figure 9). The pseudo-first-order rate constant at the maximum activity is 1.98×10^{-6} s^{-1} ([Cu] = 2[L] = [NPP] = 3 mM, pH = 8.4). This value is ca. 150-fold lower than that of BNPP under identical conditions, probably due to the two negative charges of NPP, and thus the further hydrolysis of NPP was neglected in our calculations.

The hydrolysis of BNPP by the Cu^{II}−tdci system proved to be catalytic, since, when a 10.5-fold excess of substrate over the dinuclear complex was used (2.55×10^{-4} M), nine turnovers were detected during 400 min (Figure 10). Slight product inhibition was observed during the reaction, which is probably related to the stronger complex formation properties of the NPP dianion than of the BNPP (the observed kinetic data is well modeled by considering the formation of an inactive $[Cu_2LH_{-3}(NPP)]^{-}$ complex with $K = 490$ M^{-1}).

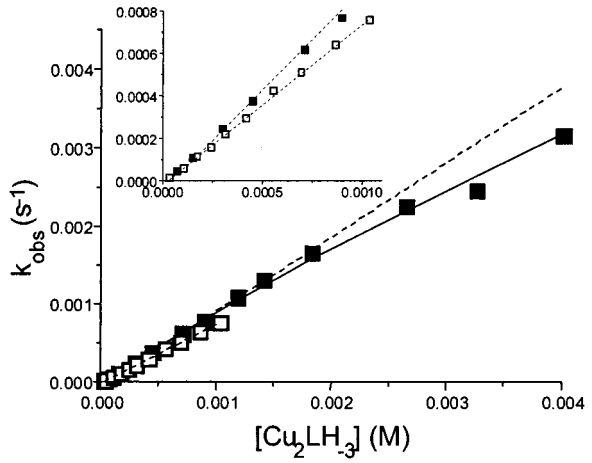

Figure 11. Dependence of the rate of BNPP hydrolysis on the concentration of the dinuclear Cu_2LH_{-3} species; $[Cu^{II}]:[L] = 2:1$, pH = 8.60, $T = 298$ K. □: [BNPP] = 1×10^{-3} M (initial slope method). ■: [BNPP] = 2×10^{-5} M (integral method).

Under optimal conditions ($[Cu^{II}]/[L] = 1.99$, pH = 8.6) the observed rate constants for the BNPP hydrolysis show first-order dependence on the concentration of the Cu_2LH_{-3} species (Figure 11), which further supports its active role in the catalysis. The second-order rate constants determined by the initial slope and integral methods are $k_2 = 0.75_6$ and 0.95_3 M^{-1} s^{-1}, respectively. These data indicate very high activity of the Cu_2LH_{-3} species. The value of k_2 is ca. 47600-fold higher than that of the hydroxide ion catalyzed hydrolysis (k_{OH}), which results in a 3.5×10^7 fold rate acceleration compared to the autohydrolysis in the presence of 4 mM dinuclear complex at pH 8.6.[28] The data presented in Figure 11 show linear dependence at lower concentration, and the onset of saturation at higher complex concentration, although complete saturation was not observed in the range of the available concentrations.[29] The limited water solubility of BNPP prevented the kinetic study under saturating substrate conditions, too. In order to achieve substrate saturation, the more water soluble 2,4-dinitrophenyl ethyl phosphate (DNPEP) was used. The hydrolysis of DNPEP, promoted by the copper(II)−tdci system, shows behavior very similar to that of BNPP, e.g., the pH−rate profiles for BNPP and DNPEP have identical shape (see Figure 9). The observed pseudo-first-order rate constants in the case of DNPEP are about the half of those with BNPP under identical conditions. This can be explained simply by statistical reasons, since DNPEP contains only one activated phosphoester bond. The observed saturation with increasing DNPEP concentration (Figure 12) strongly suggests that the hydrolysis proceeds through pre-equilibration of an active (catalyst−substrate) complex. The Michealis−Menten constant (K_M), determined by nonlinear parameter fitting, is 26.2 mM ($K_{ass} \sim 1/K_M = 38$ M^{-1}) and the first-order catalytic rate constant (k_{cat}) is 5.54×10^{-3} s^{-1}. K_M indicates moderate binding affinity of DNPEP to the dinuclear Cu_2LH_{-3} species, but the value of k_{cat} further supports the high hydrolytic activity of this complex.[10b]

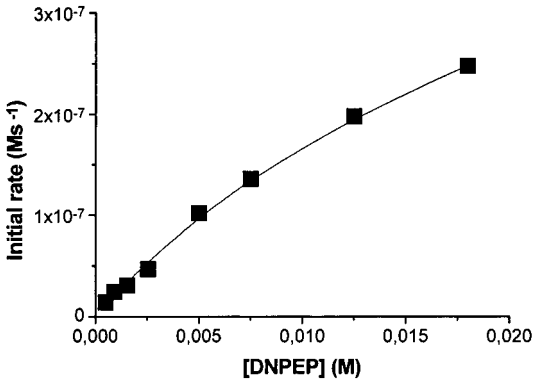

Figure 12. Dependence of the initial rate of the DNPEP hydrolysis on the substrate concentration; $[Cu_2LH_{-3}] = 1.1 \times 10^{-4}$ M, pH = 8.6, $T = 298$ K.

The above observations indicate some useful properties of the Cu^{II}−tdci system: (i) it is very efficient at hydrolyzing BNPP, and (ii) the hydrolysis in this system is catalytic and (iii) selective for the phosphodiester. To our knowledge the Cu_2LH_{-3} species is more active for BNPP hydrolysis than any other divalent metal complex, as well as most of the lanthanide(III) complexes reported to date. Only a few lanthanide(III)/H_2O_2 systems[3a] and tetravalent metal ions (Zr^{IV} and Ce^{IV})[3d,e] are more efficient. Highly active metal complexes are seldom able to discriminate between phosphomonoesters and phosphodiesters.[6a] Consequently, the rate of hydrolysis is often comparable, or even higher, for the monoester, which is unfavorable in terms of developing artificial nucleases. Furthermore, only a few highly active complexes are reported to have catalytic behavior.[3b,c]

The proposed structure of the dinuclear Cu_2LH_{-3} species (Chart 1a) contains two metal-bound hydroxide ions in addition to the bridging alkoxo group, although the alternative structure with metal-promoted deprotonation of three hydroxy groups cannot be ruled out definitively, since metal-coordinated alkoxo groups have been shown to act as efficient nucleophiles in phosphoester hydrolysis.[4] If this mechanism applied in our system, it would result in a transesterification from BNPP, leading to the formation of a new, nonactivated phosphoester derivative of tdci. Although this kind of compound should be hydrolytically inert, attempts to detect such transient species in our system using HPLC were unsuccessful. On the contrary, reverse-phase HPLC measurements confirmed the exclusive formation of *p*-nitrophenolate and *p*-nitrophenyl phosphate (NPP) during the hydrolysis of BNPP. This suggests that a hydrolytic mechanism is indeed operating, and this can involve either general-base catalysis or direct nucleophilic attack of a metal-bound hydroxide ion. Although these processes are rather difficult to differentiate, we propose intramolecular nucleophilic catalysis, based on the outstanding activity of the Cu_2LH_{-3} species.

According to the structure of $[\mathbf{1}]^{4+}$, tdci provides 3.6−3.8 Å Cu−Cu separation for the alkoxo-bridged centers, which is comparable to the distance between the two metal centers in a number of dinuclear metallophosphatases.[1] Recently, several X-ray crystallographic studies indicated that phosphodiesters are able to form μ-1,3-bridges between alkoxo-[19a] or phenoxo-bridged[30] dicopper(II) units of similar metal separation. The hydrolytic activity of the mononuclear $CuLH_{-1}$ species is negligible by comparison with that of the Cu_2LH_{-3} complex,

(28) $k_{uncat} = 9 \times 10^{-11}$ s^{-1}, calculated as a sum of the spontaneous hydrolysis (1.1×10^{-11} s^{-1}) and of the alkaline hydrolysis ($k_{OH} = 2 \times 10^{-5}$ M^{-1} s^{-1}) at pH 8.6 and 298 K: Menger, F. M.; Gan, L. H.; Johnson E.; Durst, D. H. *J. Am. Chem. Soc.* **1987**, *109*, 2800.

(29) Saturation kinetic measurements using the integral method at higher concentration of dinuclear species ($[Cu_2LH_{-3}] > 0.004$ M) were complicated by the intensive absorption of the complexes at 400 nm. Assuming Michaelis−Menten kinetics for the hydrolysis, the data in Figure 11 suggest a very high catalytic rate constant ($K_M \geq 0.024$ M, $k_{cat} \geq 0.02$ s^{-1}).

(30) Wall, M.; Hynes, R. C.; Chin, J. *Angew. Chem., Int. Ed. Engl.* **1993**, *32*, 1633.

suggesting significant cooperativity between the two metal centers. The enhanced activity is due, at least in part, to the double Lewis activation provided by the dinuclear species. In conclusion, we propose double Lewis activation with intramolecular nucleophilic catalysis for the Cu_2LH_{-3}-promoted hydrolysis of BNPP, as depicted in Chart 1b.

Activated phosphodiesters with good leaving groups, such as BNPP, are not truly adequate models for biological phosphodiester hydrolysis. However, the Cu^{II}−tdci (2:1) system also provides substantial rate acceleration for the hydrolysis of cyclic nucleotide monophosphates and dinucleotides. Studies on such systems are currently underway in our laboratory.

Conclusion

The crystalline copper(II) complex of tdci has a pentanuclear structure with an extensive hydroxo/alkoxo-bridged framework, which results in the formation of a unique Cu_5O_6 cage. In solution several mono-, di-, and trinuclear species exist, each having different deprotonation states, and the solution composition depends on both the metal-to-ligand ratio and pH. CW and pulse EPR measurements provided evidence that the Cu^{II} ion of the mononuclear complexes is directly coordinated to a nitrogen, and that strongly antiferromagnetically coupled dinuclear and EPR active trinuclear complexes exist, in agreement with the solution equilibrium data. The Cu_2LH_{-3} complex, formed around pH 8.5, is highly active for the hydrolysis of the activated phosphodiester BNPP (3.5×10^7 fold rate acceleration compared to the autohydrolysis in the presence of 4 mM dinuclear complex at pH 8.6), and the reaction was shown to be catalytic. The corresponding mononuclear complex ($CuLH_{-1}$) is virtually inactive, indicating important cooperativity between the metal centers. The proposed mechanism is a double Lewis activation with intramolecular nucleophilic catalysis.

Acknowledgment. T.G. thanks the Alexander von Humboldt Foundation for a research fellowship. This work was supported by the Deutsche Forschungsgemeinschaft, the Fonds der Chemischen Industrie, the Hungarian Research Foundation (Project No. T025114), and the Foundation of Research Developments at Universities (FKFP-0109/2000). The authors thank Dr. Roberta Sessoli (Università degli Studi di Firenze, Italy) for the magnetic measurements, Dr. Walter Amrein (ETH Zürich, Switzerland) for the FAB^+ MS spectra, Dr. Peter Osvath (CSIRO, Clayton, VIC, Australia) for his careful reading of the manuscript, Prof. Michael Veith for providing the X-ray facility, and Dr. V. Huch for the collection of the data set.

Supporting Information Available: Listings of crystallographic data (anisotropic displacement parameters, positional parameters, bond distance, and bond angles) of $[Cu_5(tdciH_{-2})(tdci)_2(OH)_2(NO_3)_2](NO_3)_4 \cdot 6H_2O$, vis spectra of the $[Cu^{II}$−tdci system, individual vis spectra of the formed di- and trinuclear complexes, EPR and ENDOR spectra. Crystallographic data in CIF format. This material is available free of charge via the Internet at http://pubs.acs.org.

IC0005902